Available online at www.sciencedirect.com
ScienceDirect
Journal of Power Sources 160 (2006) 454–461
JOURNAL OF POWER SOURCES
www.elsevier.com/locate/jpowsour

Intra-fuel cell stack measurements of transient concentration distributions

W.P. Partridge *, T.J. Toops, J.B. Green, T.R. Armstrong

Oak Ridge National Laboratory, United States

Received 31 October 2005; received in revised form 30 December 2005; accepted 5 January 2006
Available online 21 February 2006

Abstract

Intra-fuel-cell measurements are required to understand detailed fuel-cell chemistry and physics, validate models, optimize system design and control, and realize enhanced efficiency regimes; in comparison, conventional integrated fuel-cell supply and effluent measurements are fundamentally limited in value. Intra-reactor measurements are needed for all fuel cell types. This paper demonstrates the ability of a capillary-inlet mass spectrometer to resolve transient species distributions within operating polymer-electrolyte-membrane (PEM) fuel cells and at temperatures typical of solid-oxide fuel cells (SOFC). This is the first such demonstration of a diagnostic that is sufficiently minimally invasive as to allow measurements throughout an operating fuel cell stack. Measurements of transient water, hydrogen, oxygen and diluent concentration dynamics associated with fuel-cell load switching suggest oxygen-limited chemistry. Intra-PEM fuel cell measurements of oxygen distribution at various fuel-cell loads are used to demonstrate concentration gradients, non-uniformities, and anomalous fuel cell operation.

Keywords: In situ measurements; In-operando measurements; Intra-fuel-cell measurements; PEMFC; SOFC; Humidity

1. Introduction

Improved fuel cell efficiencies can be realized through detailed understanding of device chemistry and physics provided by in situ intra-reactor measurements that resolve transient species concentration distributions across and within the cells. Such species variations reflect changes in the manifold sub-processes involved in fuel cell operation; e.g., reactants and products distribution and transport, localized and possibly dynamic active-site blocking, membrane degradation, etc. In turn, such species measurements can be used to better understand and optimize the component processes. With integrated or reactor-in and -out (i.e., supply and effluent) measurements, the process can only be optimized on average. In contrast, intra-reactor measurements allow higher-order optimization throughout the fuel cell.

The need for and potential of such advanced-measurement-driven insights is recognized by the broad fuel cell community as demonstrated by the diversity of approaches for resolving various intra-reactor distributions. Nishikawa et al. used a segmented polymer electrolyte fuel cell (PEMFC) and commercially available humidity and temperature sensors to study the distribution of water transport across the membrane [1]. This transport was correlated with current density distributions, humidity, polymer membrane water content and cathode oxygen concentration. The observations allowed a better understanding of the dynamic efficiency distributions along the fuel cell flow path. Hakenjos et al. applied infrared (IR) and visible imaging techniques to a segmented PEMFC with an IR window over the anode flow path to study intra-reactor current, temperature and water distributions [2]. Through this work they associated intra-PEMFC areas of low current density with specific loss mechanisms, and suggested that through this improved knowledge optimized flow-field designs could be realized. Barreras et al. modified a commercial PEMFC to gain optical access throughout one flow path and used laser-induced fluorescence imaging to study reactant flow distributions [3]. The results were used to val-

Abbreviations: BPR, back pressure regulator; DMFC, direct methanol fuel cell; GDL, gas diffusion layer; i.d., internal diameter; IR, infrared; LHS, left-hand side; MEA, membrane electrode assembly; MFC, mass flow controller; MS, mass spectrometer; o.d., outside diameter; PEM, proton exchange membrane; PEMFC, proton exchange membrane fuel cell; RGA, residual gas analyser; RHS, right-hand side; sccm, standard cubic centimeters per minute; SOFC, solid oxide fuel cell; SpaciMS, spatially resolved capillary inlet mass spectrometer; T_{10-90}, time between the 10% and 90% response points; UHP, ultra-high purity; XAFS, X-ray absorption fine-structure spectroscopy

* Corresponding author at: Oak Ridge National Laboratory, 2360 Cherahala Blvd., Knoxville, TN 37932, United States. Tel.: +1 865 946 1234; fax: +1 865 946 1354.
E-mail address: partridgewp@ornl.gov (W.P. Partridge).

0378-7753/$ – see front matter © 2006 Elsevier B.V. All rights reserved.
doi:10.1016/j.jpowsour.2006.01.016

idate flow models, identify the source of non-uniform flow, and better understand the sources of inefficiencies. Mench et al. used gas chromatography to measure species distributions, including water, O_2 and N_2, on the anode and cathode sides of a PEMFC's 22-pass serpentine flow path. Measurements were made with 2 min temporal resolution and used to better understand the distributed nature of water transport and chemistry, and its relation to local PEMFC output [4]. Roth et al. used in situ X-ray absorption fine-structure spectroscopy (XAFS) to actively monitor the catalyst oxidation states at a select location within an operating PEMFC, and stated the importance of the technique for studying aging and deactivation processes [5]. Kramer et al. applied neutron imaging to a direct methanol fuel cell (DMFC) to study two phase flow in various flow-path geometries [6]. This work demonstrated the transient and distributed nature of mass-transport limitations, and corresponding distributions in the intra-DMFC electrochemistry efficiency. Of the works cited above, that of Kramer et al. was the least invasive and the only one that did not require direct flow-path access or invasive modifications. This diverse group of efforts not only demonstrates the need for intra-fuel cell diagnostics, but highlights the range of component processes/issues that can have distributed performance and impact the local and integrated fuel cell efficiency. All of the cited works demonstrate significant progress to better understand some component process critical to fuel cell efficiency. A common limitation of this diverse group of diagnostics for resolving intra-fuel-cell distributions is that they require end-plate access and are all limited to single cell applications; i.e., they cannot be applied to resolve inter-cell distributions. Moreover, other than the neutron imaging work [6], the cited diagnostics are of varying degrees of invasiveness. This is generally representative of fuel cell diagnostics; they are invasive and have limited ability for full-stack analysis. Improved diagnostics that are minimally invasive and allow full-stack analysis are needed to realize optimum efficiencies through better understanding of the detailed fuel cell component processes.

Although the previous examples are limited to PEMFC and DMFC devices, intra-fuel-cell and inter-stack diagnostics are needed to improve the understanding and efficiency of all fuel cell types. SOFC gas analysis is generally recognized as particularly difficult [7]. Nevertheless, advanced diagnostics have been applied to study fundamental SOFC chemistry [8–10]. The work of Finnerty et al. is particularly notable in the context of this paper in that an MS was used to resolve transient SOFC reforming and carbon deposits [10]; Finnerty's paper demonstrates the value of real-time in situ diagnostics for understanding detailed reactor chemistry, but on an integrated reactor-effluent basis. Minimally invasive intra-reactor diagnostics could extend these insights to allow the distributions of reactions within the SOFC to be studied.

Spatially resolved capillary-inlet mass spectrometry (SpaciMS) is a candidate species diagnostic for making minimally invasive intra- and inter-stack measurements within fuel cells. The instrument is based on direct capillary sampling to a residual gas analyzer; i.e., capillaries are directly mounted in the bipolar-plate channels, blocking less than 3% of the flow-path and sampling at approximately 10 μL min^{-1}. This sampling methodology is minimally invasive and enables species measurements in both single- and multi-cell configurations. Moreover, the SpaciMS measurement methodology is relatively easy to configure and implement, and thus accessible to the entire fuel-cell community.

This instrument was primarily developed to improve the understanding of the detailed chemistry and species distributions in diesel engine exhaust and catalyst systems, and has been successfully implemented into a wide range of conditions including: catalyst beds on both bench-scale [11,12] and full-engine platforms [13,14], advanced diesel combustion [15], non-reacting gas mixing [16], and electrically active non-thermal plasma reactor chemistry [17]. In these applications the SpaciMS has been configured to provide 104 ms–1 s temporal resolution (based on T_{10-90} response, i.e., time between the 10% and 90% response points), and quantify species concentrations in the 10 ppm to tens of percent ranges. Although these applications have required concentration gradients to be measured only on centimeter scales, the spatial resolution is limited only by the ability to control capillary translation; e.g., 2 mm spatial resolution should be readily feasible. The SpaciMS has provided unique detail regarding the network and sequence of catalyst chemistry, and previously unavailable insights into improving the performance efficiency of diesel-catalyst systems. Similar unique insights into fundamental fuel cell chemistry and physics are expected from SpaciMS applications.

Fuel cell applications offer several additional challenges to SpaciMS measurements compared to the primarily combustion and catalysis examples cited above. Diesel catalyst environments are typically 300–450 °C, non-condensing, with at most typically percent levels of hydrogen. For fuel cells using pure H_2, there may be challenges to measuring small concentration changes on a large baseline. High temperature, 800–1000 °C, SOFC operation will affect both the mechanical nature of the capillary physical probe, as well as the sample density and thus signal level. The condensing PEMFC environment increases the possibility of capillary probe occlusion by liquid water. The effort described here details the investigation of these issues and assesses the feasibility of SpaciMS for the described applications. This paper describes the first application of the SpaciMS for the measurement of fuel cell species transients associated with load switching, and intra-fuel-cell species distributions. Measurements are made at temperatures characteristic of PEMFC and SOFC devices to demonstrate broad instrument applicability.

2. Experimental

2.1. Fuel cell platform

A commercially available (ProFC-3, H_2 Economy) three-cell PEMFC stack, with 7 cm × 7 cm active area per cell, was used for the research described here. The graphitic bipolar plates incorporated 13-pass 918 mm long dual parallel serpentine flow channels, with crossed anode–cathode flow paths. The flow paths

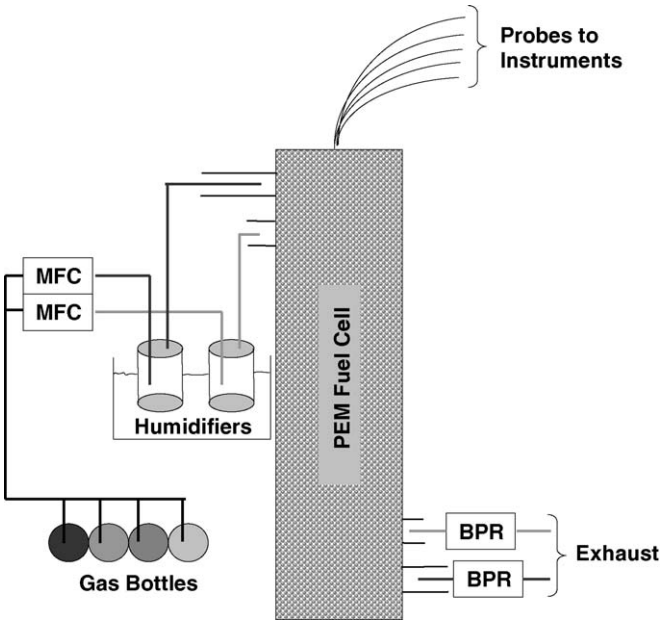

Fig. 1. Schematic of fuel-cell system.

consisted of 1.27 mm diameter half channels, with 0.633 mm^2 cross-sectional flow area. When assembled, the inlet and outlet manifolds were common for the three parallel cells.

A schematic of the fuel cell system is shown in Fig. 1. Mass flow controllers (MKS Instruments, Inc.) were used to meter bottled gas (Air Liquide, H_2: UHP, O_2: Research Grade, Ar: UHP) to the fuel cell. Reactant humidity was controlled by bubbling reactant gasses through deionized water, heated in a water bath (Neslab RTE-110). SpaciMS probes were installed at select locations throughout the anode and cathode flow paths. Back pressure regulators (Swagelok KCB1A0C5EP11) were used to operate the fuel cell at the specified pressure. The fuel cell and proximal plumbing were wrapped in heat tape, and Variacs used to control the temperature to 83 °C. A manually switched resistive load bank was used to create load variations. The anode reactant conditions were 35% H_2, 35% Ar, 30% H_2O, 22 psig; 100 sccm, 50/50 H_2/Ar dry gas mixture. The cathode reactant conditions were 14% O_2, 56% Ar, 30% H_2O, 25 psig; 100 sccm, 20/80 O_2/Ar dry gas mixture. This corresponds to an oxygen-limited equivalence ratio of 0.8 based on standard PEMFC electrochemical reactions [18].

2.2. Simulating SOFC temperatures

To investigate applicability of SpaciMS for quantifying transient species distributions at SOFC-typical temperatures, the PEMFC exhaust streams were heated to 900 °C. To heat the exhaust streams, a length of 1 mm i.d. tubing was coiled to fit a 1.3 m section within a tube furnace (Barnstead/Thermolyne 21100). Individual coiled tubes heated the anode and cathode exhaust separately. SpaciMS sample capillaries were positioned within the heated tubes to sample the exhaust streams in approximately the center of the tube furnace.

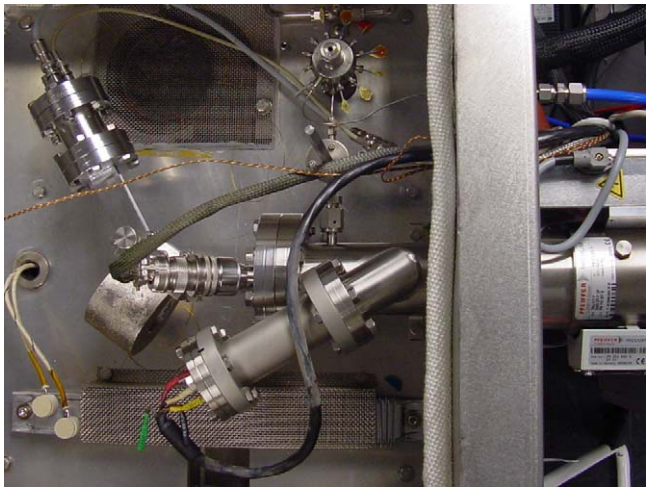

Fig. 2. Picture of SpaciMS showing heated hose (black hose in top RHS) containing sample capillaries, 12×-multi-port valve (top center), magnetic-sector RGA (LHS). The diagonal tube is the ionization gauge (center lower section).

2.3. SpaciMS and data system

The SpaciMS used in this study is shown in Fig. 2 and was based on a magnetic-sector residual gas analyzer (Vacuum Technology, Inc.) using electron ionization and equipped with an electron multiplier. Multiple fused silica capillaries (Polymicro Technologies), 1.8 m long, 50 μm i.d., 150 μm o.d., were used to transport samples at select locations throughout the fuel cell system to a multi-port valve (Valco). The sample flow rate was approximately 10 $\mu L\,min^{-1}$ for each capillary, and gases were continuously drawn through all capillaries. The electronically controlled multi-port valve was used to select the sample stream directed to the MS for analysis. The MS and multi-port valve were housed in a 95 °C oven to mitigate sample condensation and sample-instrument-wall interactions. Between the fuel cell and the heated SpaciMS, the sample capillaries were housed in heated hoses (Atmo Seal, Inc.) at 150 °C. The SpaciMS was typically operated in a selected-ion-monitoring mode, and a separate data system (National Instruments) was used to record the selected species concentrations (e.g., H_2, O_2, N_2, Ar, H_2O), fuel cell output, and SpaciMS pressure at 1 Hz. For the setup used here, the T_{10-90} response time was 1 s. This response time is dominated by broadening in the sample capillary, and can be reduced by using shorter capillaries; in other applications measurements have been made with a T_{10-90} of 100 ms. For the work reported here, the capillary length and data acquisition rate were matched and specified to the fuel cell system.

2.4. Capillary probe access

For general stream sampling outside the fuel cell, standard compression fittings (Swagelok) were used with vespel reducing ferrules. For the high-temperature measurements, the ferrules were sufficiently removed from the heated zone to satisfy specifications.

The minimally invasive nature of the SpaciMS capillary sampling probes affords intra-fuel cell measurements. Specifically, the SpaciMS sampling rate is 0.01% of the 100 sccm dry reactant flow rate per capillary, and each capillary takes up only 2.8% of the flow-channel cross-sectional area; i.e., SpaciMS is minimally invasive both in terms of sampling rate and physical-probe size. For intra-fuel-cell sampling, the capillaries were mounted in the bipolar plate parallel to a select pass (of the 13-pass serpentine) approximately 5 mm into the specific flow pass. Fig. 3a shows an instrumented bipolar plate with sampling capillaries positioned in the inlet manifold and at the 2×, 6× and 10× locations for both the anode and cathode sides; this corresponds to 0%, 15%, 46% and 78% along the serpentine flow paths. The instrumented anode and cathode flows do not correspond to the same cell for the work reported here. The nature of the dual parallel serpentine flow path is clear from Fig. 3a. The cathode flow path is the transpose of the anode flow path visible in Fig. 3a. Fig. 3b shows a close up of the capillary installation; the minimally invasive nature of the capillaries is apparent from this figure. To mount the capillaries, small grooves were milled in the bipolar plate using a router (Dremel) and the capillaries were sealed and fixed in place using silicone (GE Silicone II). The fuel cell supplier used silicone gaskets between the bipolar plates and MEA. The assembled and instrumented three-cell PEMFC is shown in Fig. 3c.

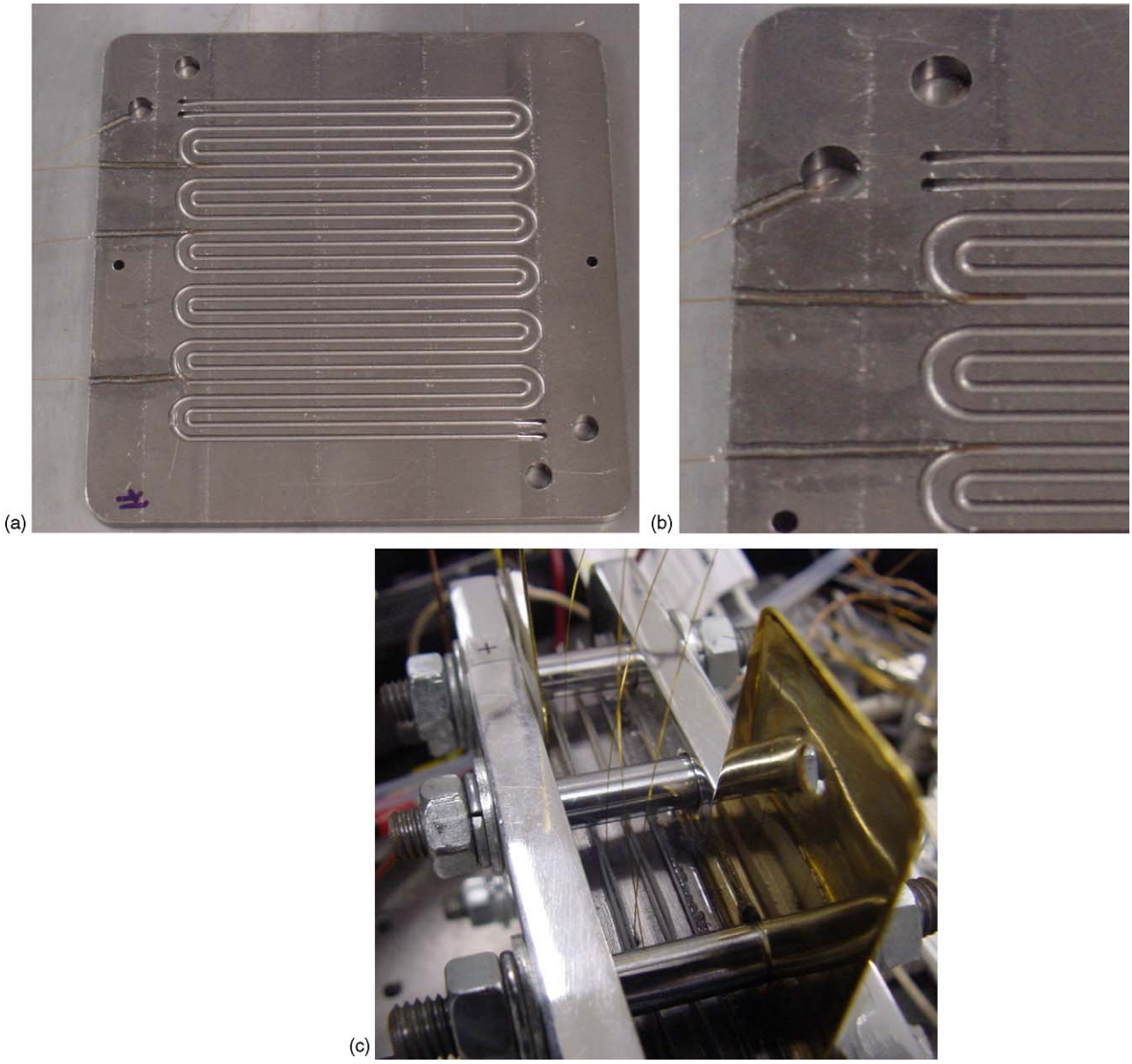

Fig. 3. (a) Dual-serpentine path bipolar plate instrumented with sample capillaries, (b) detail of capillary insertion methodology highlighting minimally invasive nature of sample-capillary scale relative to the flow-path scale, and (c) assembled three-cell fuel-cell stack with one bipolar plate instrumented for intra-reactor species measurements on both the anode and cathode sides.

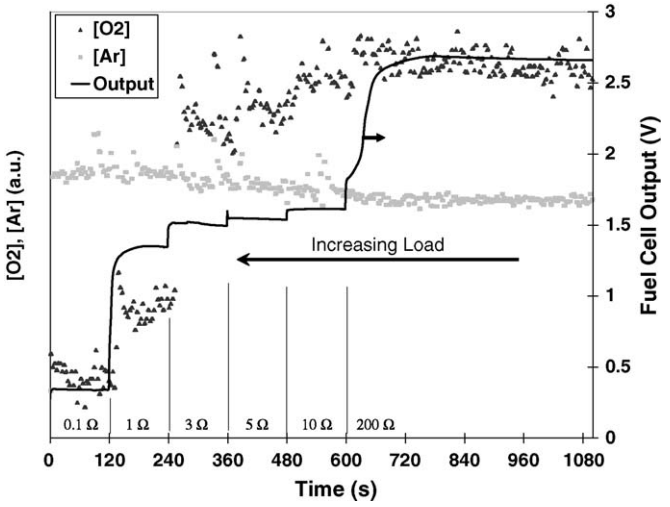

Fig. 4. Cathode-side O_2 and Ar transients associated with load switching, and corresponding fuel-cell-output transients.

3. Results and discussion

3.1. Fuel-cell-effluent transient species measurements

Measurements were made of PEMFC exhaust species concentration transients as the load was switched. Discrete external resistances were switched in the fuel cell circuit to produce load switching. Distinct step changes in H_2, O_2, H_2O and Ar concentrations were observed to accompany load step changes. Fig. 4 shows O_2 and Ar transients in the cathode effluent stream associated with load switching, and the corresponding fuel-cell-output transients. In general increasing load resulted in greater H_2 and O_2 depletion. Argon diluent concentrations increased with H_2 and O_2 consumption on both the anode and cathode sides, respectively; this expected behavior demonstrates the potential feasibility of performing major species balances. High water loading conditions could challenge the capillary sampling system resulting in partial transient capillary occlusion or in the worst case capillary clogging; transient occlusion events resulted in high frequency dynamics on the pressure and non-water species traces, and a longer-term water concentration dynamic as the excess water was removed from the capillary. Water blocking of the capillary stopped sample flow and caused the SpaciMS to go to high vacuum; this type of water clogging can often be reversed by reverse flow of inert through the sample capillary. Water-induced dynamics were most prevalent on the cathode side at high load conditions. This is expected since cathode-side water concentration should be highest at high-load conditions. Low-frequency variations in both species concentrations and fuel cell output were observed even at a steady-load condition. These are apparently due to transient local reactant depletion or passivation; e.g., local water condensation.

3.2. SOFC-temperature fuel-cell-effluent transient species measurements

Measurements of dynamic species concentrations at SOFC temperatures posed little additional challenges compared to the measurements at PEMFC temperatures. The higher temperature environment results in fewer sample molecules in the MS due to decreased sample density, and increased capillary flow resistance. These effects posed no great measurement challenge, as evidenced by the signal-to-noise ratio of the high-temperature measurements relative to the lower-temperature (PEMFC-out) measurements. Certainly at SOFC-typical temperatures quartz sample capillaries become fragile because the polyimide coating burns off at temperatures above 400 °C. This is not an issue as long as sufficient care is taken; e.g., minimize vibrations and rough surfaces and edges scoring the capillaries. No capillaries were broken in these experiments and successful implementation has been demonstrated in previous engine-based catalyst experiments where vibrations and scoring edges were prevalent.

Fig. 5a and b shows the transient species distributions associated with PEMFC load switching, with the exhaust at 900 °C and with capillaries positioned as described in Section 2.2. The load was switched every 120 s in discrete steps to ramp the output power up and down; the corresponding external resistances are

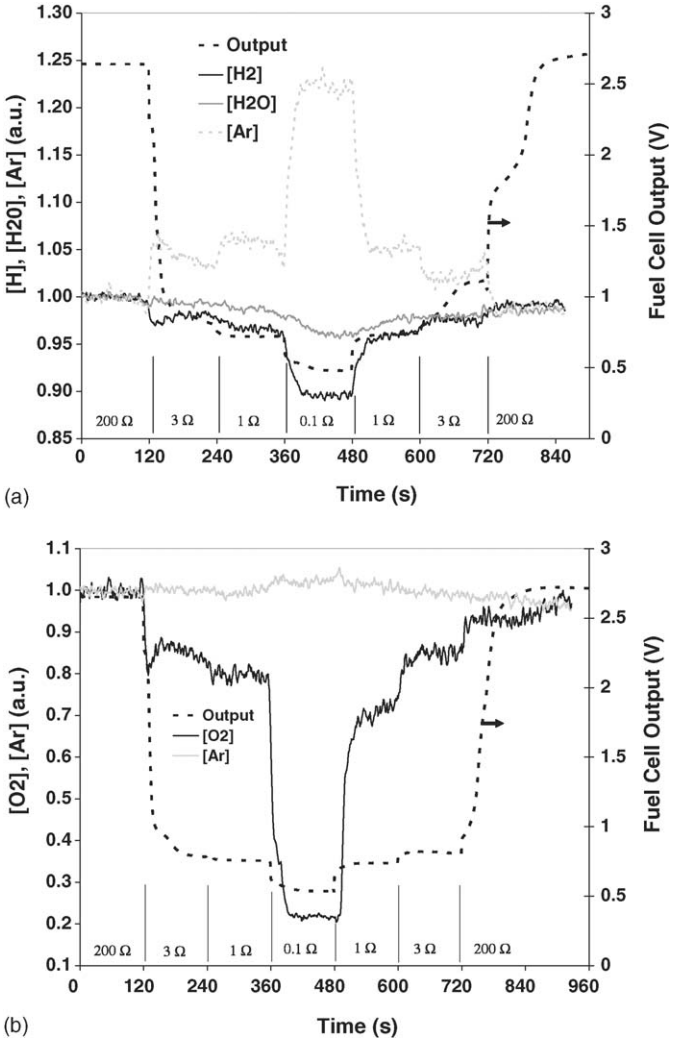

Fig. 5. (a) Transient anode species-pool dynamics, at SOFC-typical temperatures, associated with fuel-cell load switching and (b) transient cathode species-pool dynamics, at SOFC-typical temperatures, associated with fuel-cell load switching.

200, 3, 1, 0.1, 1, 3 and 200 Ω. The hysteresis in the output power is apparently in part due to changing internal resistance of the cells. Species concentrations in Fig. 5a and b are not calibrated to percent concentration values, but are shown as SpaciMS current output normalized to the value at the initial 200 Ω load.[1] What can be qualitatively assessed from the concentrations profiles in Fig. 5a and b is the direction (increasing or decreasing) and shape of the concentration dynamic associated with load switching, and the shape of a transient response normalized by the total signal change associated with the corresponding load transient. The point of these measurements was to demonstrate capability which does not require calibration; calibrated data is shown in the next section. Clear correlations between the species and output curves are apparent.

Fig. 5a anode curves show increasing H_2 and H_2O depletion with increasing load. This is consistent with basic PEMFC electrochemical reactions [18]. As with the low-temperature measurements, the Ar diluent concentration increases with H_2 and H_2O depletion, demonstrating the potential feasibility of a complete major-species balance. The output voltage consistently displays initial high-frequency and subsequent low-frequency response to step load changes; these are very distinct at the 200–3, 1–0.1 and 3–200 Ω switching points. These distinct changes in response behavior are likely indicative of changes in the fundamental rate limiting step of the fuel cell chemistry; the ultimate goal of intra-fuel-cell measurements is to better understand these changes and optimize the system accordingly. The H_2 and Ar curves show some of the transient nature of the output voltage dynamics. The H_2O depletion appears to occur more slowly compared to the H_2 and Ar dynamics. None of the anode reactants are depleted for the operational range investigated.

Fig. 5b cathode curves show increasing O_2 depletion with increasing load, and a correspondingly increasing Ar balance. Despite the O_2-lean stoichiometry of the fuel cell reactant feed, O_2 is not depleted even at the highest load, 0.1 Ω, condition. The O_2 concentration transient associated with the 1–0.1 Ω load step appears to correlate more closely with the output voltage dynamic than does the corresponding H_2 transient; specifically, a greater portion of the total step O_2 concentration change is contained in the initial high frequency dynamic than for the H_2 transient. This appears to indicate that the process is limited by O_2 at the 0.1 Ω load condition rather than H_2 limited. This also might be indicated by the slow O_2 response associated with the 3–200 Ω step at the end of the scan. In fact the cathode scan in Fig. 5b is 60 s longer than Fig. 5a anode scan because of the slow O_2 recovery. This slow recovery might be due to repopulation of the gas-diffusion layer, GDL, and membrane following operating at or near O_2 depleting conditions; remember that these experiments demonstrate SpaciMS at SOFC-typical temperatures, but that a PEMFC was used to produce the species dynamics.

At SOFC-typical temperatures the SpaciMS sample capillaries become fragile due to burning of the protective polyimide coating. In such applications, the coating would in fact be removed before operation to prevent interaction of the polyimide combustion products with the fuel cell. The fragile nature of uncoated capillaries does not preclude high-temperature applications. We have demonstrated that supported fused-silica capillaries do not mechanically deform at SOFC-typical temperatures; such support could be provided by a fuel cell wall or more robust ceramic sleeve. Moreover, these capillaries can be bent, even against sharp edges, at high temperature without breaking. The major vulnerability of these uncoated capillaries is scoring and vibration; neither of which is an issue in bench fuel cell evaluations. While care must be taken with uncoated sample capillaries associated with high-temperature applications, this does not preclude SpaciMS SOFC applications.

The high-temperature measurements demonstrate the applicability of SpaciMS to SOFC environments. Details of the transient response nature demonstrate the value of the SpaciMS for elucidating fundamental kinetic limitations in the fuel cell operation. This information could be used to improve fuel cell efficiency by optimizing operational parameters, flow-path design, GDL and membrane materials properties (e.g., diffusion rates), etc. These insights are generally available from fast fuel-cell-effluent diagnostics, and can be used to optimize a fuel cell relative to its average or integrated conditions. The limitation of this type of analysis is that the fuel cell conditions are not uniform at some average value. Rather, intra-fuel-cell conditions are distributed and dynamic. For example one of the many diffusive processes might limit the process at the flow-path front, another might be limiting further down the flow path, and one reactant might become depleted at the back of the flow path. This distributed performance can change with time; for instance, with localized and transient flooding or drying of the active sites. Without detailed knowledge of the local intra-fuel-cell conditions, the process cannot be fully optimized. Intra-fuel-cell diagnostics can provide insights for realizing new realms of efficiency improvements.

3.3. Intra-fuel-cell species distribution measurements

Intra-PEMFC species measurements were expected to be one of the most challenging SpaciMS applications due to the condensing nature of the environment; specifically, due to the possibility for capillary occlusion by condensed water. Despite initial plans to mitigate water issues by housing the sample capillary in a heated and insulated 0.5 mm o.d. sleeve, bare quartz unheated capillaries were used for the work reported here. Even in this most vulnerable sampling scenario, no water-clogging challenges were experienced with any of the intra-PEMFC capillaries. This is notable particularly because realistic water concentrations were used. In fact, the water-associated sampling challenges were strictly confined to the capillaries outside the PEMFC. Certainly, water occlusion of SpaciMS sample capillaries will present challenges in certain PEMFC conditions.

[1] Calibration factors, % amp^{-1}, are unique to each species and SpaciMS setting, so concentration changes associated with load switching are not proportional for the various species. Moreover, the anode and cathode Ar curves are not comparable because the parent ion, 40 amu, was monitored for the cathode measurements while the doubly charged ion, 20 amu, was used for the anode measurements.

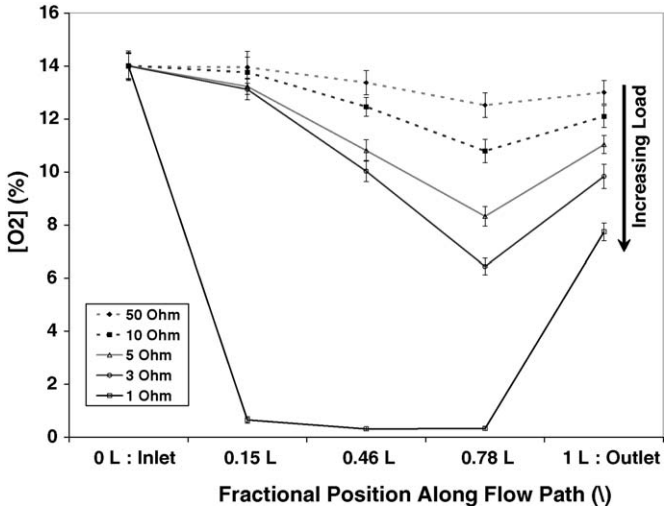

Fig. 6. In situ intra-fuel-cell measurements of O_2 distribution along the serpentine flow path at five fuel cell power levels. Uncertainty bars represent ±3-sigma noise fluctuations.

However, the highly humid PEMFC environment does not preclude intra-fuel-cell SpaciMS measurements of transient species distributions as is demonstrated below.

Intra-PEMFC SpaciMS measurements have been used to resolve localized O_2 consumption within the instrumented cell, as well as intra-cell and inter-cell non-uniformities. Fig. 6 shows the oxygen distribution through the PEMFC and the 3-sigma noise fluctuations, for five different load conditions. The 3-sigma noise is based on the sample standard deviation of approximately 49 data points; the corresponding uncertainty based on the standard deviation of the mean is indicated by the noise value in Fig. 6 divided by 7 (square root of 49). Clearly the measurement uncertainty is completely adequate to resolve the oxygen variations in Fig. 6. The measurements used capillaries installed in the fuel cell at 0L, 0.15L, 0.46L and 0.78L, where L is the serpentine path-length. The measurements at 0L used a capillary positioned in the cathode-side intake manifold, and the measurements at 1L used a capillary positioned outside the stack in the cathode exhaust stream. The loads corresponded to five fixed external resistances applied to the stack terminals; in order of increasing fuel cell output power these resistances were 50, 10, 5, 3, and 1 Ω. Fig. 6 indicates monotonically increasing oxygen consumption along the instrumented cathode flow path within the stack. At all locations the oxygen consumption increases with increasing output. For all loads investigated, the 1L (effluent) oxygen concentration is greater than that at the 0.78L (internal) location.

The increasing oxygen concentration in the exhaust relative to the 0.78L intra-fuel-cell location indicates anomalous performance behavior; either inter-cell efficiency variations and/or flow-path shorting. As mentioned earlier, these measurements were performed on one cell of a three-parallel-cell PEMFC with common inlet and exit manifolds. Separate measurements indicated no air leaks; thus, the observed phenomenon is not simply due to oxygen diffusion into the system from the surrounding atmosphere. The behavior of Fig. 6 may indicate that other parallel (not instrumented/measured) cells are less efficient than the instrumented cell; if those other cells are less efficient, they would use less oxygen than the instrumented cell and subsequently increase the oxygen concentration in the common exhaust manifold. For instance at 1 Ω and based on the 0.78L conditions, the instrumented cell appears to be exhausting 0% oxygen, but the two parallel cells may be exhausting some combination of oxygen concentration that averages to approximately 8%. This interpretation would indicate cell-to-cell non-uniformity and further demonstrates the need for intra-fuel-cell species distribution measurements. The validity of this interpretation could be assessed via cell-specific fuel cell output measurements. Alternatively, the reactants may be shorting the flow path; i.e., reactants may be flowing across the flow-path lands through the GDL rather than following the serpentine flow path. In this case, the reactants may be flowing diagonally in Fig. 3a from the inlet to outlet manifold locations. The result of flow-path shorting would be a lower reactant concentration at the serpentine path turning points, where the capillaries are positioned, compared to the flow-pass center. The validity of this interpretation could be assessed via measurements of reactant distribution along each flow-path pass. The results of Fig. 6 may be consistent with some combination of cell-to-cell non-uniformity and flow-path shorting.

Fig. 6 also shows significant oxygen consumption for the 1 Ω case, with the oxygen being depleted somewhere between the 0.15L and 0.46L locations; i.e., in this case the back 54–85% of the flow path is inactive due to an oxygen limited condition. This is a very clear demonstration of an undesirable intra-cell reactant gradient, and also demonstrates the concept of a spatially varying limiting step. Although the back end of the flow path is clearly reactant limited, the front portion has some other limiting step; e.g., oxygen diffusion to the membrane triple-phase sites, etc. This type of data can be used to design out efficiency limitations like those obvious in Fig. 6 at high load; e.g., different reactant feed concentrations and/or flowrates, graded active sites to control and distribute the reaction, alternate flow geometries, modified GDL/membrane properties to control the reaction, etc.

The high-load results of Fig. 6 are consistent with the independent high-temperature measurements of Fig. 5b. Specifically, Fig. 5b suggests that the high-load, 0.1 Ω, case was oxygen-limited although the fuel cell effluent oxygen is not depleted at this condition. We can see from the intra-fuel-cell measurements of Fig. 6 that indeed an oxygen limited condition exists at high-load operation in the instrumented cell. This produces the correlation between the O_2 and fuel cell output observed in Fig. 5b. However, this behavior is diluted by the less efficient parallel cells which on average do not consume O_2 as efficiently as the instrumented cell and/or flow-path shorting as discussed above; either or a combination of these non-uniform effects account for the lack of O_2 depletion in Fig. 5b at high load.

SpaciMS measurements of transient water concentration were demonstrated. Intra-fuel-cell water distribution measurements were also made but not reported here. These measurements can be calibrated to conventional concentration units as were the intra-fuel-cell oxygen measurements. Relative humidity is a complex parameter which combines both local water con-

centration and temperature. By combining the SpaciMS water concentration measurements with spatially resolved intra-fuel-cell temperature measurements, the transient relative humidity distributions throughout an operating fuel cell could be measured. We have recently demonstrated such measurements and will report them in a follow-on manuscript.

4. Conclusions

Fuel cell effluent measurements of transient species concentrations associated with load switching have been made at PEMFC- and SOFC-typical temperatures using the SpaciMS instrument. SpaciMS analysis is applicable to a broad range of fuel cell types. The direct capillary sampling and MS analysis of the SpaciMS instrument provide high temporal resolution and broad species applicability while being minimally invasive. Despite the challenging nature of PEMFC condensing environments to capillary sampling techniques, we were able to make in situ intra-PEMFC SpaciMS measurements at realistic humidity levels. These measurements demonstrated the relationship between fuel cell output power and oxygen consumption along the cathode serpentine flow path. Moreover, the intra-PEMFC measurements identified intra-cell concentration gradients and non-uniformities, as well as anomalous operation. At all loads the anomalous operation was indicated by a greater oxygen concentration in the common exhaust manifold than at the 0.78L intra-PEMFC location, which suggests some combination of cell-to-cell non-uniformity and/or flow-path shorting through the GDL.

Intra-fuel-cell measurements provide a more detailed understanding of the instantaneous and local chemistry and physics. This advanced understanding can allow efficiency improvements to be realized where the fuel cell process is locally optimized throughout the reactor, instead of an average or integrated basis. Intra-fuel-cell analysis allows improvements over a broad range of process components including flow-path design, reactant stream concentrations, and material formulations. Furthermore, intra-fuel-cell measurements can be used to better understand degradation processes such as start–stop and thermal cycling, effects of fuel-borne or air-borne impurities, localized drying, membrane and bipolar plate degradation, etc.

Acknowledgements

Research sponsored by the Laboratory Directed Research and Development Program of Oak Ridge National Laboratory, managed by UT-Battelle, LLC, for the U.S. Department of Energy under Contract No. DE-AC05-00OR22725.

References

[1] H. Nishikawa, R. Kurihara, S. Sukemori, T. Sugawara, H. Kobayasi, S. Abe, T. Aoki, Y. Ogami, A. Matsunaga, J. Power Sources 155 (2006) 213–218.
[2] A. Hakenjos, H. Muenter, U. Wittstadt, C. Hebling, J. Power Sources 131 (2004) 213–216.
[3] F. Barreras, A. Lozano, L. Valino, C. Marin, A. Pascau, J. Power Sources 144 (2005) 54–66.
[4] M.M. Mench, Q.L. Dong, C.Y. Wang, J. Power Sources 124 (2003) 90–98.
[5] C. Roth, N. Martz, T. Buhrmester, J. Scherer, H. Fuess, Phys. Chem. Chem. Phys 4 (2002) 3555–3557.
[6] D. Kramer, E. Lehmann, G. Frei, P. Vontobel, A. Wokaun, G.G. Scherer, Nuclear Inst. Methods Phys. Res. A 542 (2005) 52–60.
[7] N.Q. Minh, J. Am. Ceram. Soc. 76 (1993) 563–588.
[8] H.F. Poulsen, S. Garbe, T. Lorentzen, D.J. Jensen, F.W. Poulsen, N.H. Andersen, T. Frello, R. Feidenhas'l, H. Graafsma, J. Synchrotron Rad. 4 (1997) 147–154.
[9] L. Sorby, F.W. Poulsen, H.F. Poulsen, S. Garbe, J.O. Thomas, Mater. Sci. Forum 278–281 (1998) 408–413.
[10] C.M. Finnerly, R.H. Cunningham, R.M. Ormerod, Catal. Lett. 66 (2000) 221–226.
[11] J.S. Choi, W.P. Partridge, C.S. Daw, Appl. Catal. A 293 (2005) 24–40.
[12] J.S. Choi, W.S. Epling, N.W. Currier, W.P. Partridge, Catal. Today 114 (2006) 102–111.
[13] W.P. Partridge, J.M.E. Storey, S.A. Lewis, R.W. Smithwick, G.L. DeVault, M.J. Cunningham, N.W. Currier, T.M. Yonushonis, SAE Trans: J. Fuels Lubricants 109 (2000) 2992–2999.
[14] B. West, S. Huff, J. Parks, S. Lewis, J.-S. Choi, W. Partridge, J. Storey, SAE Trans: J. Fuels Lubricants 4 (2004) 1975–1985.
[15] J. Parks, S. Huff, J. Pihl, J.S. Choi, B. West, SAE International 2005 01-3876, 2005.
[16] W.P. Partridge, S.A. Lewis, M.J. Ruth, G.G. Muntean, R.C. Smith, J.H. Stang, SAE Trans.: J. Engines 111 (2002) 2699–2704.
[17] Privately reported work with Atmospheric Glow Technologies (http://www.atmosphericglow.com) to characterize the intra-reactor transient species distributions of a low-temperature plasma reactor, 2001.
[18] Fuel Cell Handbook, 7th ed. National Technical Information Service, U.S. Department of Commerce, 5285 Port Royal Road, Springfield, VA, 2004.